ELSEVIER

Catalysis Today 31 (1996) 65–77

CATALYSIS TODAY

# Hydrogenation/dehydrogenation of polycyclic aromatic hydrocarbons using ammonium tetrathiomolybdate as catalyst precursor

Richard P. Dutta *, Harold H. Schobert

*Fuel Science Program, 209 Academic Projects Building, The Pennsylvania State University, University Park, PA 16802, USA*

**Abstract**

The hydrogenation and dehydrogenation behavior of naphthalene, phenanthrene, and pyrene using ammonium tetrathiomolybdate as a catalyst precursor were investigated via their product distribution and kinetic/thermodynamic parameters. Hydrogenation reactions were carried out in 25 ml microautoclave reactors at 350, 400, and 450°C for various times up to equilibrium conditions. A lumped kinetic model was used to determine forward and reverse rate constants, which were then used to determine Arrhenius parameters. Enthalpy data were obtained and compared to values calculated in the literature. It was found that the temperature where dehydrogenation of hydroaromatics became favorable over hydrogenation reactions decreased with increasing ring size. This was also shown by an increasing thermodynamic control over the reactions as ring size increased.

*Keywords:* Hydrogenation; Dehydrogenation; Polycyclic aromatic hydrocarbons; Ammonium tetrathiomolybdate as catalyst precursor

## 1. Introduction

Coal liquefaction can be considered a technically viable alternative for the production of liquid transportation fuels if the coal macromolecule can be broken up into low molecular weight fragments, and the fragments can then be hydrogenated to decrease the concentration of aromatics and heteroatoms (nitrogen, sulfur, and oxygen) in the final product. The liquefaction process can be facilitated using various sulfided catalysts, which are generally resistant to poisoning by heteroatomic compounds. Derbyshire [1,2] and Mochida et al. [3] have reviewed the extensive literature on this subject. Research by McMillen et al. [4–6] has brought about a greater understanding of the hydrogen-transfer mechanism involved in the coal dissolution process. However, the exact role of the catalyst is still under question. The catalyst is thought not to participate in bond cleavage directly. The breaking of these bonds in the coal macromolecule is generally considered to be a thermally driven process. However, the use of a catalyst, along with a hydrogen-donor solvent, does improve conversion to liquid products. In fact, if the coal is relatively easy to convert, a catalyst will improve conversion even without a good donor solvent being present [7]. Therefore,

* Corresponding author.

0920-5861/96/$32.00 
*PII* S0920-5861(96)00084-3

research into catalyst development and the effects of catalysts on coal dissolution and upgrading of primary products is an important component of coal liquefaction development.

Molybdenum has long been a focus of research into catalytic coal liquefaction. In a recent historical essay, Moulijn and colleagues have traced the use of sulfided molybdenum catalysts for coal conversion back at least to 1924 [8]. The use of dispersed molybdenum catalyst in a pilot plant has been reported by Moll and Quarderer [9]. Liquefaction improves with an increase in molybdenum concentration, but limits have been observed beyond which further increases in molybdenum addition no longer have a significant effect [10–12]. Because the catalytically active form, $MoS_2$, is insoluble, a dispersion of molybdenum onto coal particles is often effected using so-called catalyst precursors. The precursors are soluble compounds of molybdenum that may have little or no catalytic activity themselves but are presumed to convert to a catalytically active form at liquefaction temperatures. Ammonium heptamolybdate (AHM) has been used in liquefaction research [1,13,14]. Derbyshire [1], Moulijn et al.[8], and Weller and Pelioetz [14] produced ammonium tetrathiomolybdate (ATTM) by sulfiding AHM with $H_2S$. They observed higher conversions using this precursor instead of AHM. The mechanism by which ATTM decomposes to its active form, $MoS_2$, has been studied by Prasad et al. [15], and later by Naumann et al. [16]. The latter work describes the decomposition of ATTM to amorphous $MoS_2$ in the temperature range of 350–450°C. Work by Romanowski and Roczniki discusses the rapid decomposition of ATTM under hydrogen atmosphere [17].

In our laboratory, the most recent work showing the effectiveness of ATTM in coal liquefaction is that by Burgess [18] and by Huang [7]. Through careful coal selection, it was shown that coal conversions of up to 95% could be achieved in catalytic reactions, although the hexane-soluble oils produced in the process still remained aromatic. The aromatics in the coal liquids have to be removed if they are to be used for liquid transportation fuels. In the United States, the 1990 Clean Air Act amendments have significantly restricted the allowable concentrations of aromatic compounds in gasoline and diesel fuels [19]. Coal may be the preferred feedstock for advanced generation jet fuels that would be able to withstand severe thermal stressing without decomposing to carbonaceous solids. However, aromatics have been shown to be precursors to solid deposition in fuels at elevated temperatures [20–22]. Upgrading processes would have to be employed to hydrogenate the aromatics produced during liquefaction. This step would involve catalytic hydrotreating of the primary liquid products from coal. However, if capital investment and operating costs of a coal-to-liquids plant are to be kept to a minimum, it would be advantageous to hydrogenate as many of the coal fragments as possible during the liquefaction step itself; that is, as the coal fragments are released during the depolymerisation of the coal macromolecule.

Various strategies have been formulated for application of temperature during liquefaction. These strategies are concerned with optimizing depolymerisation of coal, upgrading primary products, and avoiding retrogressive reactions. The retrogressive reactions represent the recombination of reactive free radicals to form a carbonaceous char that resists further reaction. Such reactions are often the result of the fact that the rate of hydrogenation – specifically, hydrogen capping of free radicals generated from thermal cleavage of coal macromolecules – cannot catch up to that of free radical formation. In temperature-staged and temperature-programmed liquefaction, a low-temperature pretreatment stage is followed by a high-temperature reaction stage. Conditions during the second stage are responsible for the quality of the coal liquids produced. With careful 'fine tuning' of the reaction conditions, it could be possible to have advantageous thermodynamics in the system along with a reasonably fast rate

of depolymerisation of the coal macromolecule. Basically, a trade-off between reaction kinetics and thermodynamics is possible.

Because of the complexity of the macromolecular structures of coals, the likely existence of numerous parallel reactions during liquefaction, and the production of dozens of individual compounds in the coal-derived liquids, research into the effect of various reaction conditions is facilitated by model compounds. Hydrogenation of aromatics has been studied for many years and the available literature is vast. It has been reviewed by Moreau and Geneste [23], Girgis and Gates [24], and Stanislaus and Cooper [25]. The research has focused on kinetic, thermodynamic and product distribution analysis. Correlations among the reactivities of two-, three-, and four-ring compounds are lacking. Recently, Korre et al. [26] studied the hydrogenation of aromatics using $CoMo/Al_2O_3$ as catalyst. Categories of naphthalenic and phenanthrenic hydrogenations were introduced and comparisons of their kinetic data and equilibria were given.

This paper will discuss the hydrogenation and dehydrogenation reactions of naphthalene, phenanthrene and pyrene using ATTM as a catalyst precursor. The motivation for this work stems from previous work in our laboratory on the behavior of a variety of polycyclic compounds, aimed at investigating some of the fundamental chemical processes involved in various aspects of fuel utilization. These include direct coal liquefaction [7,18], stability of aviation fuels [20–22], and carbonization or graphitization reactions leading to carbon materials [27]. Recent work on the liquefaction behavior of resinite during coal liquefaction [28,29] also motivated the present research on model compound hydrogenation and dehydrogenation.

## 2. Experimental

All reactions were carried out in 25 ml microautoclave reactors (made of type 316 stainless steel). In all runs, $3 \pm 0.01$ g reactant (Aldrich, 99%, used as received) and $0.075 \pm 0.005$ g ammonium tetrathiomolybdate (Aldrich, 99%, used as received) were loaded into the reactor. The reactor was purged with hydrogen twice, before the final pressurization with hydrogen to 7.2 MPa (5:1 hydrogen/reactant molar ratio). Heating was accomplished by lowering the reactor into a fluidized sand bath preheated to the desired temperature. The reactor was agitated during the course of the reaction to increase contact of the reactant with the catalyst, and increase the rate of bulk hydrogen transfer through the reacting medium. After a measured reaction time, the reactor was removed from the sandbath and quenched to room temperature by immersing it in a cold water bath. The products from the reaction were removed from the reactor using tetrahydrofuran (THF). The THF was removed by rotary evaporation and the product was weighed. It was found that in all cases the mass balance of reactants and products exceeded 98%. The products were dissolved in acetone and analysed using a Perkin-Elmer 8500 gas chromatograph (column used was 30 m × 0.25 mm i.d. fused silica capillary column (DB-17) coated with 50% phenyl–50% methylpolysiloxane with a coating film thickness of 0.25 μm). Identification of the products was achieved using a Hewlett-Packard 5890II gas chromatograph coupled with a HP 5791A mass selective detector.

In order to determine the dehydrogenation behavior of the hydrogenated pyrenes, the products from pyrene hydrogenated at 350°C and 60 min, 400°C and 80 min, and 450°C and 40 min, were catalytically dehydrogenated under $N_2$. This was accomplished using the same reactors as in the hydrogenation step. The products from the three hydrogenations listed above were weighed into the reactor along with a 1 wt% (metal) loading of ATTM. The reactor was pressurised with approximately 3 MPa $N_2$ and immersed in a sandbath at the desired temperature and for the desired reaction time. After this time, the reactor was quenched as before, and

the products were removed using THF. The products were analysed using GC as before. The dehydrogenation behavior of tetralin was investigated in a similar way to the hydrogenated pyrenes.

## 3. Kinetic and thermodynamic modelling

### 3.1. Kinetic model

We begin with the simple equation considering an equilibrium between aromatics and hydroaromatics:

$$\text{Aromatics} + n\text{H}_2 \rightleftharpoons \text{Hydroaromatics} \quad (1)$$

Eq. (1) is the basis for calculating the reaction kinetics.

The rate expression is given by:

$$-\text{d}[\text{A}]/\text{d}t = k_\text{f}[\text{A}]P_{\text{H}_2}^n - k_\text{r}[\text{HA}] \quad (2)$$

where $k_\text{f}$ and $k_\text{r}$ are the forward and reverse rate constants, respectively, and $P_{\text{H}_2}$ is the hydrogen partial pressure. [A] and [HA] are the concentrations of aromatiics and hydroaromatics, respectively.

To simplify the system, two assumptions were made. (1) The forward reaction is pseudo-first-order. A reduction in hydrogen pressure is expected to occur during the reaction as aromatics are converted to hydroaromatics. However, the authors feel that because of the low activity of the catalyst for hydrogenation, this decrease is not enough to undermine any qualitative conclusions that are drawn from this simplified kinetic model. Experimentation has shown that for a drop of 100 psi $H_2$, the rate constant will decrease by 10%. Error analyses of the calculated rate constants are shown on the Arrhenius plots for each reactant. (2) The reverse reaction is first order in hydroaromatics.

Assumption 1 is introduced, and Eq. (2) becomes:

$$-\text{d}[\text{A}]/\text{d}t = k'_\text{f}[\text{A}] - k_\text{r}[\text{HA}] \quad (3)$$

where $k'_\text{f}$ is the pseudo-first order rate constant.

At equilibrium $k'_\text{f}[\text{A}] = k_\text{r}[\text{HA}]$, and therefore:

$$k'_\text{f}/k_\text{r} = [\text{HA}]_\text{eq}/[\text{A}]_\text{eq} \quad (4)$$

Also, a mass balance gives:

$$[\text{A}]_t + [\text{HA}]_t = [\text{A}]_\text{eq} + [\text{HA}]_\text{eq} \quad (5)$$

Therefore, using Eqs. (4) and (5), Eq. (3) can be rearranged to give:

$$-\text{d}[\text{A}]/\text{d}t = k'_\text{f}(1 + [\text{A}]_\text{eq}/[\text{HA}]_\text{eq})([\text{A}]_t - [\text{A}]_\text{eq}) \quad (6)$$

By putting $k_\text{obs} = k'_\text{f}(1 + [\text{A}]_\text{eq}/[\text{HA}]_\text{eq})$, and integrating, the final expression becomes:

$$\ln [\text{A}]_t - [\text{A}]_\text{eq}/[\text{A}]_0 - [\text{A}]_\text{eq} = -k_\text{obs}t \quad (7)$$

Therefore a plot of Eq. (7), gives a slope $= -k_\text{obs}$, and therefore:

$$k'_\text{f} = k_\text{obs}/(1 + [\text{A}]_\text{eq}/[\text{HA}]_\text{eq})$$

$$k_\text{r} = k_\text{f}[\text{A}]_\text{eq}/[\text{HA}]_\text{eq} \quad (8)$$

### 3.2. Determination of Arrhenius parameters

The Arrhenius equation can be used to determine how the rate constants vary with temperature. By plotting ln $k_\text{f}$ and ln $k_\text{r}$ vs. reciprocal temperature, the apparent activation energies for hydrogenation and dehydrogenation can be obtained. Also, the intersection of the two lines is the point where the rates of hydrogenation and dehydrogenation are equal. This is the boundary beyond which unfavorable dehydrogenation conditions predominate over favorable hydrogenation conditions.

### 3.3. Discussion of mass-transfer limitations

A discussion of the mass-transfer limitations on any catalytic process is warranted when considering variations in kinetic parameters. Mass-transfer limitations can be checked in the reaction system by the apparent activation energies obtained by calculation. Values below 6 kcal/mol are suspect and can mean mass-transfer is controlling the reaction to some extent.

Also, mass-transfer can be inferred in a reaction system where conversion is not linear to catalyst concentration. In this study, mass transfer limitations were checked by varying the catalyst/reactant ratio for pyrene hydrogenation. Conversion was compared at 1.3, 2.6, 5.3, and 13% ATTM/pyrene ratio. The pyrene concentration was linear in catalyst concentration for all loading ratios. This result suggests that mass-transfer limitations on this system are negligible. In a similar study, Johnston [30] showed a similar relationship between catalyst/reactant ratio and conversion, and attributed this to a reaction system that was not mass-transfer limited. However, more experimentation is necessary to determine quantitatively the effect of bulk hydrogen transfer through the reacting medium. For example, varying the agitation rate of the reactor during hydrogenation should highlight any changes in conversion due to any mass-transfer effects.

## 4. Thermodynamic calculations

$$K_p = [HA]_{eq}/[A]_{eq}1/P_{H_2}^n \quad (10)$$

where $n$ is the number of moles of hydrogen added in a given reaction, e.g. naphthalene + $2H_2 \rightarrow$ tetralin ($n = 2$); phenanthrene + $4H_2 \rightarrow$ octahydrophenanthrene ($n = 4$).

Using the van't Hoff isochore equation [Eq. (11)]

$$\mathrm{d}\ln K_p/\mathrm{d}T = \Delta H/RT^2 \quad (11)$$

the enthalpy of hydrogenation for each reaction can be calculated.

## 5. Results and discussion

### 5.1. Naphthalene hydrogenation / dehydrogenation

Fig. 1 shows how naphthalene conversion varies as a function of time at three temperatures. Tetralin was the only hydrogenation product observed. This behavior is consistent with literature reports citing the relative ease of hydrogenation to tetralin but much greater difficulty of proceeding to the decalins [31,32]. Cracking or isomerisation products of tetralin were seen at 450°C, but the total concentration did not exceed 5 wt%. At 400 and 450°C, equilibrium was reached after 60 min reaction time. Total conversion is only slightly better at 400°C. At 350°C, the reaction does not reach equilibrium; after 180 min, the conversion reached 72%. To calculate the equilibrium composition of the reaction at 350°C, an extrapolation was used to find the point of 95% conversion.

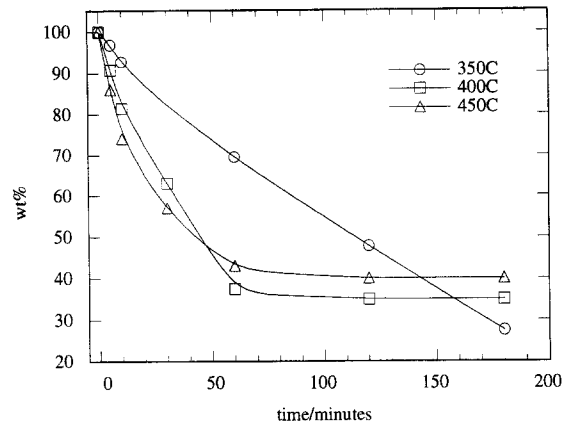


Fig. 1. Effect of temperature on naphthalene to tetralin conversion during hydrogenation.

In order to determine why only a 5% increase in conversion is seen between 450 and 400°C, the equilibrium composition of the naphthalene/tetralin/hydrogen reaction system was calculated using Gibbs free energy values from the Texas A&M University thermochemical database (5:1 hydrogen/reactant molar ratio was used in the calculation). At 350°C, equilibrium composition was calculated to be 98% tetralin and 2% naphthalene. At 400°C, values were 84% tetralin and 16% naphthalene. At 450°C, values were 64% tetralin and 36% naphthalene. Therefore, the experimental values agree quite well with the theoretical values at 350 and

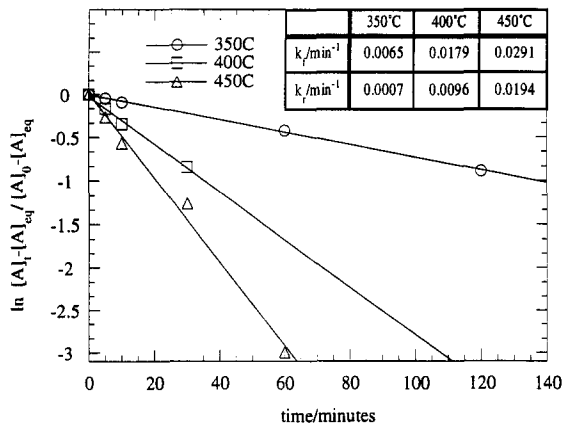


| | 350°C | 400°C | 450°C |
|---|---|---|---|
| $k_f$/min$^{-1}$ | 0.0065 | 0.0179 | 0.0291 |
| $k_r$/min$^{-1}$ | 0.0007 | 0.0096 | 0.0194 |

Fig. 2. Naphthalene hydrogenation kinetics at 350, 400 and 450°C.

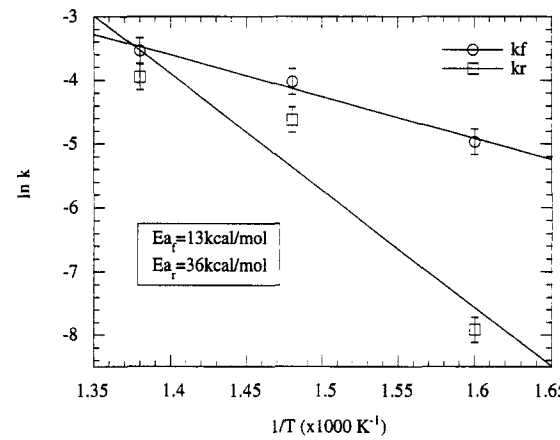


Fig. 3. Naphthalene hydrogenation/dehydrogenation Arrhenius plot.

450°C. However, conversion at 400°C is 19% less than expected from theoretical calculations. Reasons for this could be experimental error in the hydrogenation of naphthalene at 400°C. The sandbath temperature may have been higher than 400°C. Also, mass-transfer limitations could have reduced the overall conversion. However, mass-transfer did not appear to limit conversion at 350°C, a temperature at which bulk hydrogen transfer through the reacting medium would be slower.

Fig. 2 shows a kinetic plot of Eq. (7) for naphthalene hydrogenation. It can be seen that the data fit the model well. Using Eqs. (8) and (9), rate constants were calculated, and these are reported in Fig. 2. The fig. shows that as temperature increases, $k_f$ increases. The dehydrogenation rate constant also increases with increasing temperature, but the activation energies of the two reactions are different. Fig. 3 shows an Arrhenius plot for naphthalene hydrogenation/dehydrogenation. From regression analysis, calculated apparent activation energy for the forward reaction is 13 kcal/mol, and activation energy for the reverse reaction is 36 kcal/mol (these values show that the reaction rate is not controlled by mass-transfer processes). Fig. 3 also shows that dehydrogenation becomes the favorable reaction above 450°C.

To confirm this observation experimentally, tetralin was catalytically dehydrogenated under nitrogen atmosphere at 350, 400 and 450°C. Fig. 4 shows the product distribution. It can be seen that at 350 and 400°C (30 min reaction), conversions of tetralin to naphthalene are 10 and 20%, respectively. At 450°C, conversion increases to 55%, for the same reaction time. Therefore, these data confirm that dehydrogenation is the major reaction only at high temperatures (> 450°C). This has also been shown in our laboratory with research on the thermal stability of tetralin. It was shown that tetralin was stable to decomposition and dehydrogenation at 450°C [33].

The use of tetralin as a donor solvent in coal extraction and liquefaction has been studied in

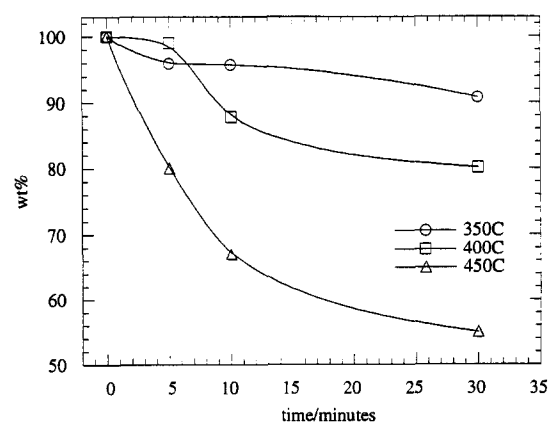


Fig. 4. Effect of temperature on tetralin to naphthalene conversion during dehydrogenation.

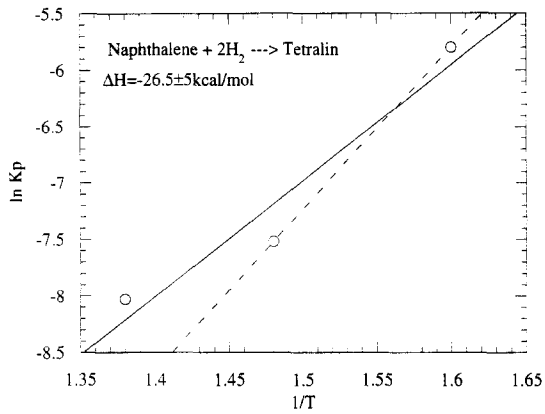


Fig. 5. Van't Hoff plot of naphthalene hydrogenation.

detail for many years. A comprehensive review of the earlier work is given by Kiebler [34]. Several useful but more recent studies are also available [35–38]. Data derived by Hooper et al. [37] show that formation of naphthalene from tetralin only occurs at temperatures greater than 435°C, and shows a pronounced increase in dehydrogenation at 450°C. These results agree quite well with the earlier work of Peter, who found tetralin decomposition up to 38% for reactions at 440°C and 1 h [39]. The reaction rate is slower than the present work because these authors used only thermal (i.e. non-catalytic) conditions. However, the thermodynamic behavior (conversion) is similar to that seen from the data obtained in the present study. It can be argued that the point where the hydrogenation and dehydrogenation rate constants are equal is the temperature that a H-donor solvent is most effective. This would be about 450°C for the naphthalene/tetralin system.

Fig. 5 shows a van't Hoff plot for hydrogenation of naphthalene to tetralin. Because of the uncertainty of behavior at higher temperatures, and uncertainties about the run at 400°C, two lines were plotted. One included the data at 450°C, and the other did not. Therefore a range of values was obtained. $K_p$ values were calculated using Eq. (10). Eq. (11) was used to calculate the enthalpy of hydrogenation. A range of $-25 \pm 5$ kcal/mol is obtained from Fig. 5. The value is in reasonable agreement with literature values of $-29.8$ and $-32$ kcal/mol [40,41].

If hydroaromatics are to be produced from aromatics, two factors have to be considered, conversion and length of time to reach the desired conversion level. As can be seen from the data, conversion decreases with increasing temperature, but the kinetics of the reaction are slower at lower temperatures. From the data, it can be concluded that high temperatures are desirable for the first 40 min of reaction, but after this time, thermodynamics limit the conversion. At this point, it is then advisable to reduce the temperature to below 400°C, and continue to convert naphthalene to tetralin, as can be seen in the reaction at 350°C. To hydrogenate only at 350°C would take too long to achieve respectable conversion. These results suggest that a concept of 'reverse temperature staging', in which an initial, high-temperature stage is followed by a second, low-temperature reaction stage, may be of benefit in achieving high yields of hydrogenated products from the liquefaction step itself.

### 5.2. *Phenanthrene hydrogenation / dehydrogenation*

Fig. 6a, b and c show the product distributions for phenanthrene hydrogenation at 350, 400 and 450°C, respectively. They show decreasing conversion as temperature increases. Also, product selectivity differs in the three different temperature reactions. At 350°C, the major primary product is dihydrophenanthrene (DHPh). Tetrahydrophenanthrene (THPh) is also a primary product, while octahydrophenanthrene (OHPh) is a hydrogenation product of DHPh and THPh. However, a maximum in the concentration of DHPh appears after 50 min reaction. The concentration then decreases from 28 to 19 wt%. This can be attributed to the dehydrogenation pathway of DHPh to phenanthrene. This was confirmed by hydrogenating DHPh at 350°C using ATTM. Fig. 7 shows that

phenanthrene is the major product during this reaction. Comparing the product distribution of THPh and OHPh with that of the same compounds shown in Fig. 6a, it can be concluded

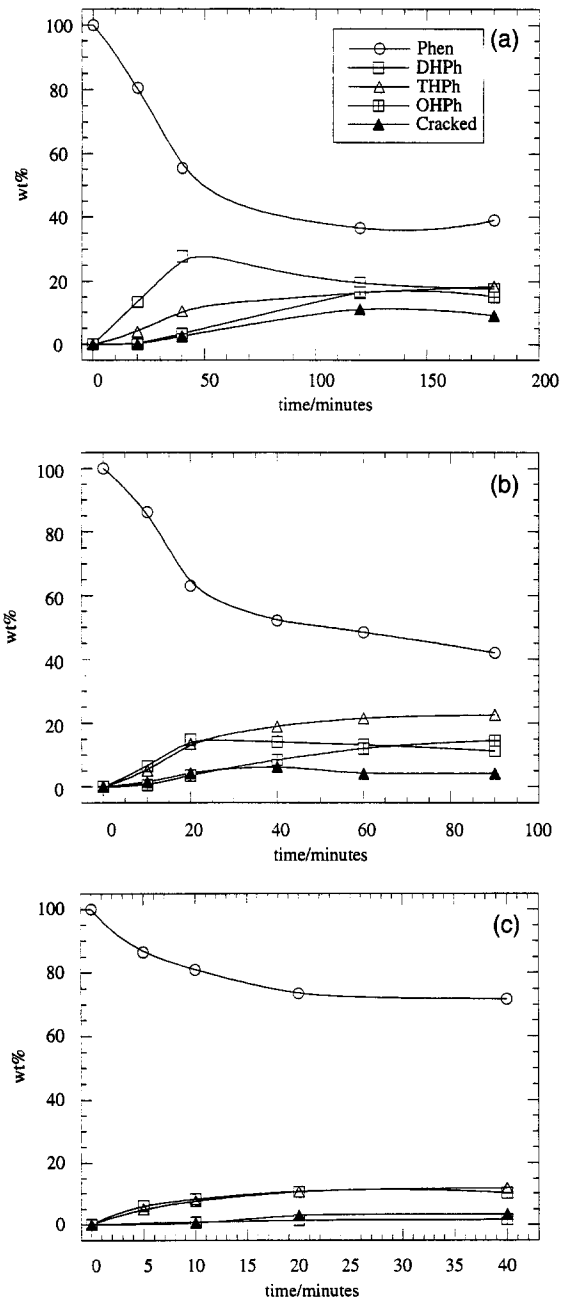


Fig. 6. (a) Phenanthrene hydrogenation product distribution at 350°C. (b) Phenanthrene hydrogenation product distribution at 400°C. (c) Phenanthrene hydrogenation product distribution at 450°C.

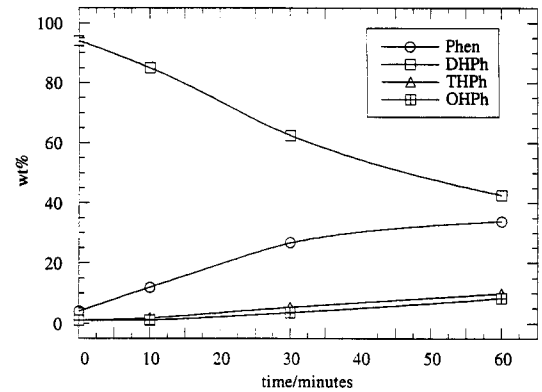


Fig. 7. Dihydrophenanthrene hydrogenation product distribution at 350°C.

that THPh is a direct hydrogenation product of phenanthrene, and OHPh is a hydrogenation product of DHPh. The interconversion of DHPh and THPh [42] seems unlikely based upon the fact that the concentration of THPh is the same when phenanthrene and DHPh are used as reactants. OHPh concentration is higher when DHPh is used as the reactant, suggesting that DHPh hydrogenates to OHPh directly.

At 400°C, the concentration of DHPh reaches a maximum in 30 min less time than at 350°C. This is due to greater reaction rates at the higher temperature, and unfavorable thermodynamics allowing dehydrogenation to take place more readily. At 450°C, dehydrogenation is the most favorable reaction and therefore conversion is limited to only 27%.

Fig. 8 shows a kinetic plot of Eq. (7) for phenanthrene hydrogenation. Pseudo-first order rate constants reported in Fig. 8 show that as temperature increases, $k_f$ increases. The dehydrogenation rate constant, $k_r$, also increases with increasing temperature, but the activation energies of the two reactions are different. Fig. 9 shows an Arrhenius plot for phenanthrene hydrogenation/dehydrogenation. From regression analysis, calculated activation energy for the forward reaction is 7 kcal/mol, and activation energy for the reverse reaction is 23 kcal/mol. These values are low but this may be attributed to the unusually high dehydrogenation suscepti-

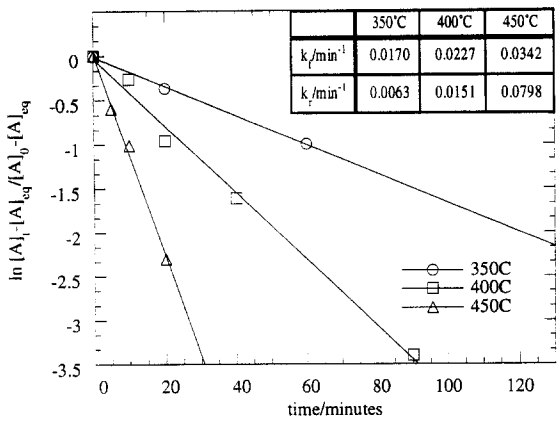


Fig. 8. Phenanthrene hydrogenation kinetics at 350, 400 and 450°C.

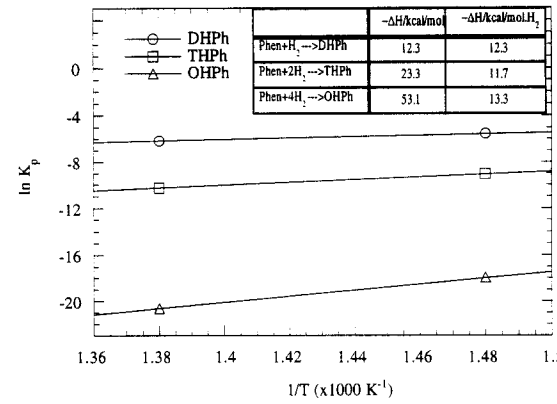


Fig. 10. Van't Hoff plot of phenanthrene hydrogenation.

bility of DHPh. It may also show that the reaction is partly controlled by diffusion processes. The crossover temperature where dehydrogenation becomes the favorable reaction is 404°C.

Fig. 10 shows a van't Hoff plot for hydrogenation of phenanthrene to DHPh, THPh and OHPh. $K_p$ values were calculated using Eq. (10). Data for the reaction at 350°C were not included because the susceptibility of DHPh toward dehydrogenation caused considerable uncertainty in the results. Eq. (11) was used to calculate the enthalpies of hydrogenation, and these are reported in Fig. 10. It can be seen that the value of $\Delta H$ per mole of hydrogen added is almost constant for the three reactions, and that the value of $-12.3$ kcal/mol (for the predominant reaction of phenanthrene + $H_2 \rightarrow$ DHPh) compares well with values given in the literature ($-12$ kcal/mol) [43].

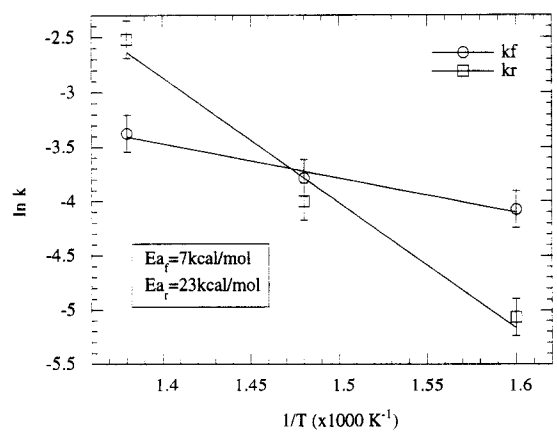


Fig. 9. Phenanthrene hydrogenation/dehydrogenation Arrhenius plot.

Thermodynamics appear to play a more important part in the hydrogenation of phenanthrene than for naphthalene. The temperature limit for favorable conditions is much lower than for naphthalene at 404°C. Also, the difference in reaction kinetics is not so pronounced as temperature increases from 350 to 400°C. The reaction rate of naphthalene hydrogenation increased almost by a factor of three, whereas phenanthrene reaction rate increased by only a factor of 1.2. These observations are in agreement with the conclusions of Girgis and Gates [24] that 'equilibrium considerations take on increasing importance with an increasing number of rings in fused-ring aromatics'.

### 5.3. Pyrene hydrogenation / dehydrogenation

Fig. 11a, b and c show the product distributions for pyrene hydrogenation at 350, 400 and 450°C, respectively. The major product at all temperatures is dihydropyrene (DHPy). Secondary hydrogenation products are tetrahydropyrene (THPy) and hexahydropyrene (HHPy). Conversion decreases as temperature

increases as seen with the other compounds in this investigation. The product selectivity at 350 and 400°C is similar except that at 350°C the hydrogenation of DHPy to THPy is allowed to continue after 80 min reaction time. Therefore, it can be seen that dehydrogenation reactions are limiting conversion at 400°C. At 450°C, conversion of pyrene stops after 20 min, with only 27% conversion to hydroaromatics.

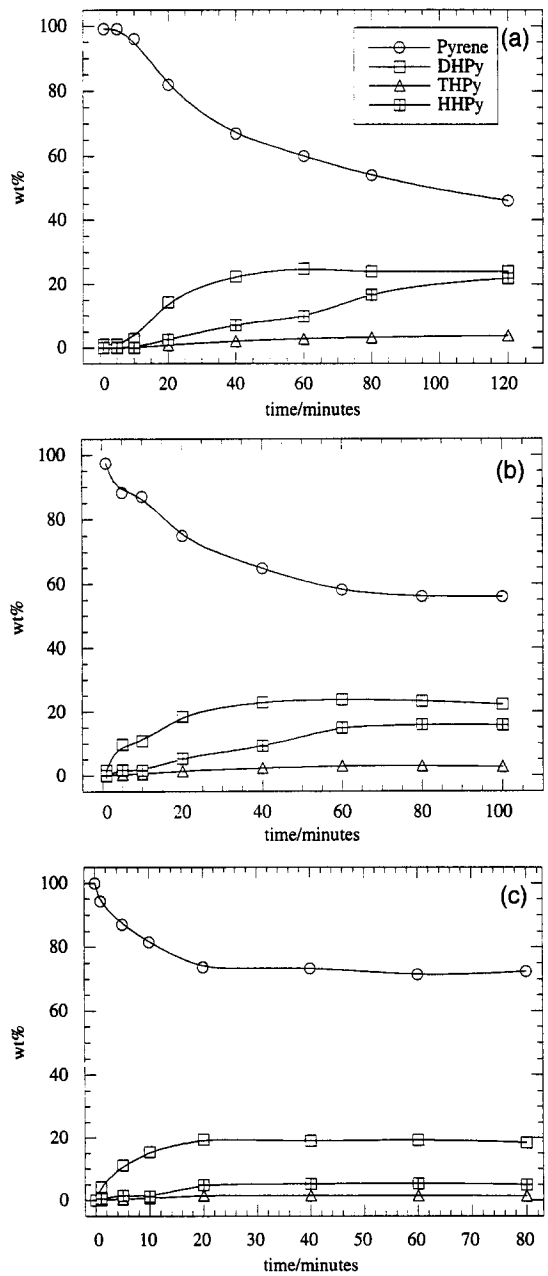


Fig. 11. (a) Pyrene hydrogenation product distribution at 350°C. (b) Pyrene hydrogenation product distribution at 400°C. (c) Pyrene hydrogenation product distribution at 450°C.

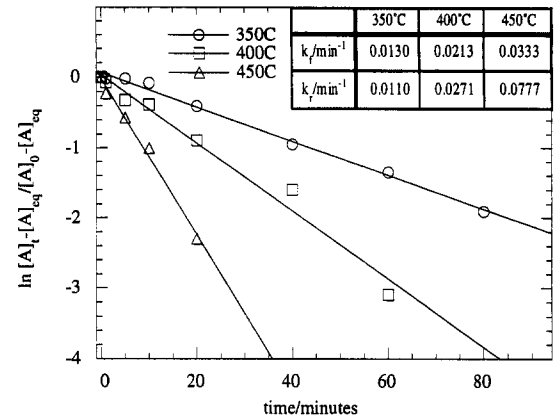


| | 350°C | 400°C | 450°C |
|---|---|---|---|
| $k_f$/min$^{-1}$ | 0.0130 | 0.0213 | 0.0333 |
| $k_r$/min$^{-1}$ | 0.0110 | 0.0271 | 0.0777 |

Fig. 12. Pyrene hydrogenation kinetics at 350, 400 and 450°C.

Fig. 12 shows a kinetic plot of Eq. (7) for pyrene hydrogenation. The pseudo-rate constants were calculated from the plot, and these are reported in Fig. 12. In a similar study by Stephens and Chapman [44], a forward rate constant of 0.019 $min^{-1}$ was obtained using a kinetic model based on pseudo-first order kinetics. Our value of 0.013 $min^{-1}$ compares reasonably well with this value, even though the hydrogen/pyrene molar ratio was much larger than in this study. This does suggest that the

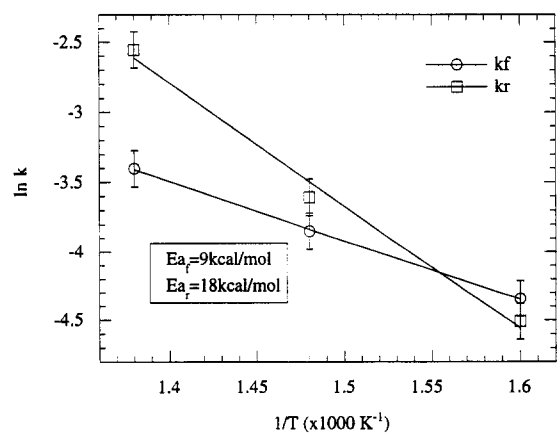


Fig. 13. Pyrene hydrogenation/dehydrogenation Arrhenius plot.

pseudo-first order kinetic model used in this study is justifiable.

Fig. 13 shows an Arrhenius plot for pyrene hydrogenation/dehydrogenation. From regression analysis, calculated apparent activation energy for the forward reaction is 9 kcal/mol, and activation energy for the reverse reaction is 18 kcal/mol. Fig. 13 also shows that dehydrogenation becomes the favorable reaction above 372°C.

In order to confirm this dehydrogenation behavior, hydrogenated pyrenes were subjected to dehydrogenating conditions, and the concentration of pyrene was followed. Fig. 14 shows that as temperature increases the amount of dehydrogenation increases. However, in contrast to tetralin dehydrogenation, lower temperatures do have a considerable effect on the dehydrogenation rate.

The use of pyrene as a hydrogen shuttler has received some attention in the literature [30,38,45–47]. In essence, a hydrogen shuttler is a compound that is easily hydrogenated by gaseous hydrogen, and easily transfers the acquired hydrogen to coal or coal-derived fragments in a subsequent process. Study of the hydrogenation/ dehydrogenation behavior of pyrene and hydropyrenes (particularly dihydropyrene) is a vital step in determining the

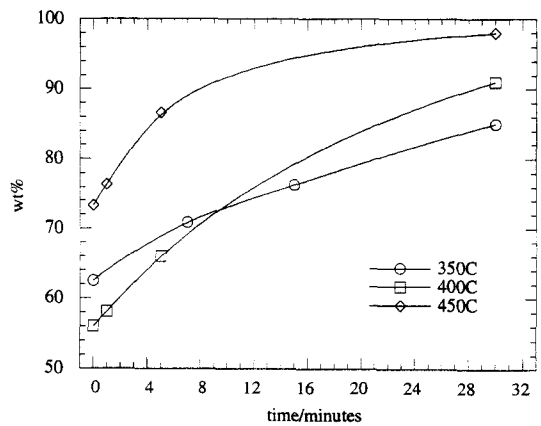


Fig. 14. Effect of temperature on hydrogenated pyrenes to pyrene conversion during dehydrogenation.

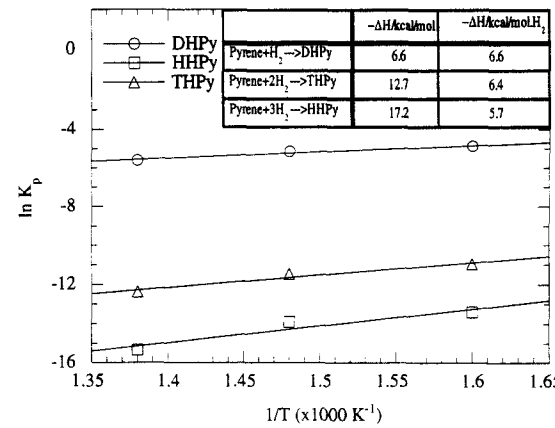


Fig. 15. Van't Hoff plot of pyrene hydrogenation.

overall effectiveness of pyrene or similar heavy aromatics as components of coal liquefaction solvents. The present work shows that hydropyrenes are susceptible to dehydrogenation at temperatures above 372°C. Therefore, because coal liquefaction is usually carried out at higher temperatures than this, the important consideration is not the ability of hydrogenated pyrenes to give up their hydrogen, but it is the hydrogenation reactivity of pyrene itself that will determine the effectiveness of the solvent.

Fig. 15 shows a van't Hoff plot for hydrogenation of pyrene to DHPy, THPy and HHPy. The enthalpies of hydrogenation are reported in Fig. 15. The values for $\Delta H$ per mole of hydrogen added are almost constant for the three reactions, and the value of $-6.6$ kcal/mol (for the predominant reaction of pyrene $+ H_2 \rightarrow$ DHPy) compares reasonably well with values given in the literature ($-10$ kcal/mol) [30].

Dehydrogenation reactions of pyrene hydroaromatics predominate above 372°C. Therefore when optimising conditions for hydrogenation of pyrene, the most important variable to take into account is the temperature. Reaction rate does not play an important role in the reaction, except for the early stages of conversion (first 20 min of reaction). These observations satisfy the earlier statement that equilibrium considerations increase with increasing ring size.

## 6. Conclusions

The main objective for this work was to be able to make comparisons for 2, 3, and 4-ring systems and try to extrapolate this behavior to larger ring systems. From a kinetic standpoint, it appears that the rate of reaction is most important for bicyclic compounds. As ring size increases, kinetics play a less important role, and thermodynamics becomes the driving force for the outcome of the reaction. In fact, the data for pyrene shows that even at the low temperature of 372°C, dehydrogenation reactions predominate. This would imply that if even larger ring systems are hydrogenated, equilibrium considerations will become even more important.

This shift in relative importance of thermodynamic and kinetic considerations can be attributed in part to the heats of formation of the various polycyclic compounds and their hydrogenated species. Shaw et al. [48] have reported these values. Fig. 16 shows a comparison of enthalpy data from the present work and Shaw et al.'s data. It can be seen that there is a good correlation between the data. Fig. 16 also shows the following thermodynamic trends. When adding 1 mol $H_2$, dihydrophenanthrene is more readily formed than dihydropyrene. When adding 2 mol $H_2$, tetrahydronaphthalene is more readily formed than tetrahydrophenanthrene, which is more readily formed than tetrahydropyrene.

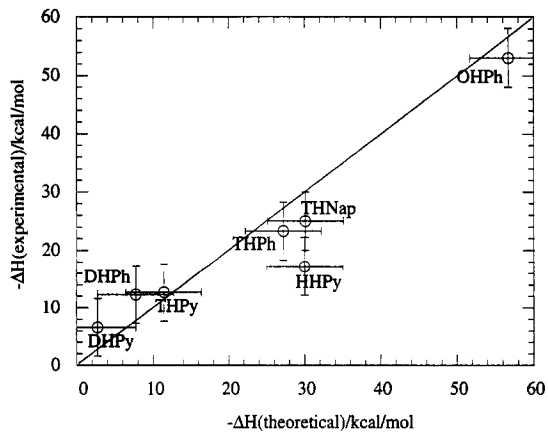


Fig. 16. Comparison of $-\Delta H_{\text{hydrogenation}}$ from present work with theoretical data [48].

In terms of coal liquefaction, temperature effects are very important when hydrogenating three- and four-ring systems, whereas the kinetics of hydrogenation of two-ring systems are very important. Therefore, a trade-off between kinetics, thermodynamics and product selectivity is necessary. A significant question to be asked when determining a coal liquefaction process is the type of product that is required. If it is desired to convert coal not simply to a synthetic crude oil, but rather to some specific product slate, then the coal has to be selected on a basis of its molecular architecture. For example, a product that requires a large concentration of tetralin and decalin, a coal-derived jet fuel for example, would need a feedstock in which bicyclic components dominate in its structure. Conditions for liquefaction can then be determined to match the desired reaction chemistry of the selected feedstock. Data from this work suggest that the important factor will be depolymerisation kinetics, and subsequent hydrogenation kinetics. A product that requires larger ring structures as part of its composition would require a coal that has these large polycyclic moieties as part of its structure. Our data suggest that if hydrogenation of the fragments is to take place, the temperature of the reaction would have to be selected carefully. A possible reaction strategy for consideration in the future, particularly for direct production of high yields of hydroaromatic or fully hydrogenated compounds, would be a reverse temperature program that would have a low-temperature final stage to avoid dehydrogenation reactions.

## Acknowledgements

This project was supported by the US Department of Energy, Pittsburgh Energy Technology Center, and the Air Force WL/Aero Propulsion and Power Directorate, Wright-

Patterson AFB. The assistance of Dr. Semih Eser with an understanding of the kinetic and thermodynamic results is greatly appreciated.

## References

[1] F.J. Derbyshire, Catalysis in Coal Liquefaction: New Directions for Research, IEA Coal Research, London, IEA CR/08, 1988.
[2] F. Derbyshire, Energy Fuels, 3 (1989) 273.
[3] I. Mochida and K. Sakanishi, D.D. Eley, H. Pines and W.O. Haag, Editors, Advances in Catalysis, Vol. 40, Academic Press, San Diego, CA, 1994, p. 39
[4] D.F. McMillen, R. Malhotra, S.-T. Chang and S.E. Nigenda, Am. Chem. Soc., Div. Fuel. Chem., 30(4) (1985) 297.
[5] D.F. McMillen, R. Malhotra, G.P. Hum and S.-J. Chang, Energy Fuels, 1 (1987) 193.
[6] D.F. McMillen, R. Malhotra, S.-J. Chang, W.C. Ogier, S.E. Nigenda and R.H. Fleming, Fuel, 66 (1987) 1611.
[7] L. Huang, Ph.D. Dissertation, The Pennsylvania State University, University Park, PA, 1995.
[8] J.A. Moulijn, P.W.N.M. van Leeuwen and R.A. Santen, in J.A. Moulijn, P.W.N.M. van Leeuwen and R.A. Santen, Editors, Catalysis: An Integrated Approach to Homogeneous, Heterogeneous and Industrial Catalysis, Elsevier, Amsterdam, 1993, Chap. 1.
[9] N.G. Moll and G.J. Quarderer, Chem. Eng. Prog., 75(11) (1979) 46.
[10] F.J. Derbyshire, V.H.J. de Beer, G.M.K. Abotsi, A.W. Scaroni, J.M. Solar and D.J. Skrovanek, Appl. Catal., 27 (1986) 117.
[11] G.M.K. Abotsi, Ph.D. Dissertation, The Pennsylvania State University, University Park, PA, 1987.
[12] A.B. Garcia and H.H. Schobert, Coal Prepr., 7 (1989) 47.
[13] S.W. Weller, Fourth International Conference on the Chemistry and Uses of Molybdenum, 1982.
[14] S.W. Weller and M.G. Pelioetz, Ind. Eng. Chem., 43(5) (1951) 1243.
[15] T.P. Prasad, E. Diemann and A.J. Muller, Inorg. Nucl. Chem., 35 (1973) 1895.
[16] A.W. Naumann, A.S. Behan and E.M. Thorsteinson, Fourth International Conference on the Chemistry and Uses of Molybdenum, 1982, p. 313.
[17] W. Romanowski and E. Roczniki, Chem. II Ann. Soc. Chim. Poionorum., 37 (1963) 1077.
[18] C. Burgess, Ph.D. Dissertation, The Pennsylvania State University, University Park, PA, 1994.
[19] National Research Council. Coal: Energy for the Future, National Academy Press, Washington, 1995.
[20] C. Song, Y. Peng, H. Jiang and H.H. Schobert, Prepr. Pap. Am. Chem. Soc., Div. Pet. Chem., 37 (1992) 484.
[21] C. Song and P.G. Hatcher, Prepr. Pap. Am. Chem. Soc., Div. Pet. Chem., 37 (1992) 529.
[22] C. Song, S. Eser, H.H. Schobert and P.G. Hatcher, Energy Fuels, 7 (1993) 234.
[23] C. Moreau and P. Geneste, in J.B. Moffat, Editor, Theoretical Aspects of Heterogeneous Catalysis, Van Nostrand Reinhold, New York, 1990, p. 256.
[24] M.J. Girgis and B.C. Gates, Ind. Eng. Chem. Res., 30 (1991) 2021.
[25] A. Stanislaus and B.H. Cooper, Catal. Rev.-Sci. Eng., 36(1) (1994) 75.
[26] S.C. Korre, M.T. Klein and R.J. Quann, Ind. Eng. Chem. Res., 34 (1995) 101.
[27] J.V. Atria, M.S. Thesis, The Pennsylvania State University, University Park, PA, 1994.
[28] R.P. Dutta and H.H. Schobert, Am. Chem. Soc., Div. Fuel. Chem., 38 (1993) 1140.
[29] R.P. Dutta and H.H. Schobert, in K. Anderson and J. Crelling, Editors, Amber, Resinite, and Fossil Resins, ACS Symp. Ser., 617 (1995).
[30] K.P. Johnston, Fuel, 63 (1984) 463.
[31] F.G. Bordwell, Organic Chemistry, Macmillan, New York, 1963, Chap. 15.
[32] R.Q. Brewster, Organic Chemistry, Prentice-Hall, Englewood Cliffs, NJ, 1953, Chap. 31.
[33] H.H. Schobert, Advanced Thermally Stable Jet Fuel development Program Annual Report, Volume II, Fuel Science Program, The Pennsylvania State University, Interim Report for Period July 1990–July 1991, p. 8.
[34] M.W. Kiebler, in H.H. Lowry, Editor, Chemistry of Coal Utilization, Wiley, New York, 1945, Chap. 19.
[35] J.M.L. Penninger, Int. J. Chem. Kinet., 14 (1982) 761.
[36] J.J. de Vlieger, A.P.G. Kieboom and H. van Bekkum, Fuel, 63 (1984) 334.
[37] R.J. Hooper, H.A.J. Battaerd and D.G. Evans, Fuel, 58 (1979) 132.
[38] B.C. Bockrath, M.L. Gorbaty, J.W. Larsen and I. Wender, Editors,, Coal Science, Vol. 2, Academic Press, New York, 1983, p. 65
[39] I. Peter, Technika, 19 (1938) 193.
[40] D.M. Speros and F.D. Rossini, J. Phys. Chem., 64 (1960) 1723.
[41] C.G. Frye and A.W. Weitkamp, J. Chem. Eng. Data., 14 (1969) 372.
[42] J.L. Lemberton and M. Guisnet, Appl. Catal., 13 (1984) 181.
[43] C.G. Frye, J. Chem. Eng. Data., 7 (1962) 592.
[44] H.P. Stephens and R.N. Chapman, Prepr. Pap. Am. Chem. Soc., Div. Fuel. Chem., 28 (1983) 161.
[45] R.C. Neaval, Fuel, 55 (1976) 263.
[46] I. Mochida, A. Takarabe and K. Takeshita, Fuel, 58 (1979) 17.
[47] F.J. Derbyshire and D.D. Whitehurst, Fuel, 60 (1981) 655.
[48] R. Shaw, D.M. Golden and S.W. Benson, J. Phys. Chem., 81 (1977) 1716.